

Zinc(II) and Copper(II) Complexes of Pentacoordinating (N₄S) Ligands with Flexible Pyrazolyl Arms: Syntheses, Structure, and Redox and Spectroscopic Properties

Sudeep Bhattacharyya,[†] Sujit Baran Kumar,^{†,‡} Subodh Kanti Dutta,[†]
Edward R. T. Tiekink,[§] and Muktimoy Chaudhury^{*,†}

Department of Inorganic Chemistry, Indian Association for the Cultivation of Science,
Calcutta 700 032, India, and Department of Chemistry, The University of Adelaide,
Adelaide, South Australia 5005, Australia

Received May 16, 1995[⊗]

Zinc(II) and copper(II) complexes of two new potentially pentadentate ligands based on methyl 2-aminocyclopent-1-ene-1-dithiocarboxylate with pendent pyrazolyl groups (Me₂pzCH₂)₂NC₂H₃RNHC₅H₆CSSCH₃ (R = H, **Hmmpcd**, and R = CH₃, **Hmmpcd**, both having N₄S donor atoms set) have been reported. The molecular structures of [Zn(mmpcd)]ClO₄ (**1b**) and [Cu(mmpcd)]ClO₄ (**2b**) show a distorted trigonal bipyramidal geometry for the Zn(II) ion and a square pyramidal geometry for the Cu(II) ion. **1b** crystallizes in the triclinic space group *P*1̄, *a* = 9.900(3) Å, *b* = 15.379(5) Å, *c* = 8.858(2) Å, α = 99.93(2)°, β = 93.62(2)°, γ = 100.38(2)°, *V* = 1300.5(7) Å³, and *Z* = 2; while **2b** crystallizes in the monoclinic space group *P*2₁/*n*, *a* = 12.859(6) Å, *b* = 12.642(3) Å, *c* = 16.503(2) Å, β = 102.67(2)°, *V* = 2617(1) Å³, and *Z* = 4. The structures were refined to final *R* = 0.042 for **1b** and 0.049 for **2b**. The EPR and electronic spectroscopic studies showed that the copper(II) species doped into zinc(II) complex adopts the zinc(II) trigonal bipyramidal structure. The cyclic voltammetric measurements indicated one-electron reversible reduction of the copper(II) complex occurring at -0.74 V, while irreversible oxidation to copper (III) takes place at +0.75 V (*vs* Ag/AgNO₃).

Introduction

Coordination chemistry of zinc has attracted much attention as increasing number of hydrolytic enzymes and DNA binding proteins have been identified in recent years with Zn(II) in their active centers.^{1,2} These biologically active zinc sites are capable of executing highly efficient and kinetically rapid catalytic reactions, possibly due to their variability and flexibility in coordination behavior.³ Attempts to understand the detailed reaction mechanisms at these zinc-binding centers, including the exact nature of metal coordination environments, are only partially successful in spite of several spectroscopic and crystallographic investigations undertaken currently with many of these enzymes.¹ Coordination environments involving nitrogen (imidazolyl) and oxygen (aqueous) with infrequent presence of sulfur (cysteinal) have been proposed for zinc in these enzymes,^{1–4} many of which form five-coordinate trigonal bipyramid zinc substrate complexes in the *entatic state*^{3a,5,6} during their turnovers. The putative five-coordinated intermediates that control the stereochemistry and dynamics of reactions are often not accessible for detailed structural studies. This has prompted several recent studies aiming to understand the

structural features of pentacoordinated zinc complexes with biologically relevant ligands as synthetic analogues.^{7–12} In these complexes zinc coordination sites are predominantly occupied by nitrogen donor atoms either solely^{7,8} or in combination with oxygen,⁹ barring a couple of reports of exclusive oxygen coordination.¹⁰ Steric environments around zinc in these complexes are largely trigonal bipyramidal (tbp)^{7,9,10} with occasional departures to square pyramidal (sp) form,⁸ entangled by distortions by varying degrees appearing almost as regular feature.

Unlike N/O coordination, reports of structurally characterized pentacoordinated zinc(II) complexes of biomimetic ligands involving sulfur donor sites are surprisingly very few in number,^{11,12} although presence of cysteinal sulfur in zinc biochromophores has been known for many years.^{3a,4} In this paper we have embarked upon the synthesis and characterization

[†] Indian Association for the Cultivation of Science.

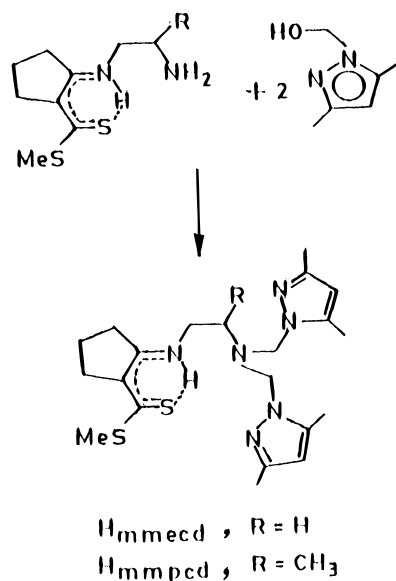
[‡] Present address: Departament de Química Inorgànica, Universitat de Barcelona, Diagonal 647, Barcelona 08028, Spain.

[§] The University of Adelaide.

[⊗] Abstract published in *Advance ACS Abstracts*, February 1, 1996.

- (1) (a) Spiro, T. G., Ed. *Zinc Enzymes*; Wiley: New York, 1983. (b) Bertini, I.; Luchinat, C.; Maret, W.; Zeppezauer, M. *Zinc Enzymes*; Birkhäuser: Boston, MA, 1986. (c) Vallee, B. L.; Galdes, A. *Advances in Enzymology*; Wiley: New York, 1984; Vol. 56, p 283.
- (2) Berg, J. M. *Science (Washington, D.C.)* **1986**, *232*, 485.
- (3) (a) Williams, R. J. P. *Pure Appl. Chem.* **1982**, *54*, 1889. (b) Prince, R. H.; Wolley, P. R. *Angew. Chem., Int. Ed. Engl.* **1972**, *11*, 408.
- (4) Corwin, Jr., D. T.; Koch, S. A. *Inorg. Chem.* **1988**, *27*, 493 and references therein.
- (5) Christianson, D. W.; Lipscomb, W. N. *Proc. Natl. Acad. Sci. U.S.A.* **1986**, *83*, 7568.
- (6) Merz, Jr., K. M.; Hoffmann, R.; Dewar, M. J. S. *J. Am. Chem. Soc.* **1989**, *111*, 5636.
- (7) (a) Adam, K. R.; Arshad, S. P. H.; Baldwin, D. S.; Duckworth, P. A.; Leong, A. J.; Lindoy, L. F.; McCool, B. J.; McPartlin, M.; Taylor, B. A.; Tasker, P. A. *Inorg. Chem.* **1994**, *33*, 1194. (b) Andres, A.; Bazzicalupi, C.; Bencini, A.; Bianchi, A.; Fusi, V.; Garcia-Espana, E.; Paoletti, P.; Valtancoli, B. *Inorg. Chem.* **1994**, *33*, 617. (c) Bencini, A.; Bianchi, A.; Garcia-Espana, E.; Mangani, S.; Micheloni, M.; Orioli, P.; Paoletti, P. *Inorg. Chem.* **1988**, *27*, 1104. (d) Takahashi, K.; Nishida, Y.; Kida, S. *Bull. Chem. Soc. Jpn.* **1984**, *57*, 2628. (e) Harrison, P. G.; Begley, M. J.; Kakabhai, T.; Killer, F. J. *Chem. Soc., Dalton Trans.* **1986**, 929. (f) Ray, N.; Hathaway, B. J. *J. Chem. Soc., Dalton Trans.* **1980**, 1105. (g) Casella, L.; Silver, M. E.; Ibers, J. A. *Inorg. Chem.* **1984**, *23*, 1409. (h) Kirchner, C.; Krebs, B. *Inorg. Chem.* **1987**, *26*, 3569. (i) Korp, J. D.; Bernal, I.; Merrill, C. L.; Wilson, L. J. *J. Chem. Soc., Dalton Trans.* **1981**, 1951.
- (8) (a) Grant, S. J.; Moore, P.; Omar, H. A. A.; Alcock, N. W. *J. Chem. Soc., Dalton Trans.* **1994**, 485. (b) Shionoya, M.; Ikeda, T.; Kimura, E.; Shiro, M. *J. Am. Chem. Soc.* **1994**, *116*, 3848.
- (9) (a) Kimura, E.; Koike, T.; Toriumi, K. *Inorg. Chem.* **1988**, *27*, 3687. (b) Kato, M.; Ito, T. *Inorg. Chem.* **1985**, *24*, 509.
- (10) (a) Grewe, H.; Udupa, M. R.; Krebs, B. *Inorg. Chim. Acta* **1982**, *63*, 119. (b) Nakacho, Y.; Misawa, T.; Fujiwara, T.; Wakahara, A.; Tomita, K. *Bull. Chem. Soc. Jpn.* **1976**, *49*, 595.
- (11) Goedken, V. L.; Christoph, G. G. *Inorg. Chem.* **1973**, *10*, 2316.
- (12) Zhang, C.; Chadha, R.; Reddy, H. K.; Schrauzer, G. N. *Inorg. Chem.* **1991**, *30*, 3865.

Scheme 1



of pentacoordinated zinc complexes in N/S donor environments as part of our ongoing studies on the chemistry of transition metal complexes in biologically relevant sulfur donor environments.^{13–18} Two new potentially pentadentate ligands, methyl ((2-(β-bis((3,5-dimethylpyrazol-1-yl)methyl)amino)ethyl)amino)cyclopent-1-ene-1-dithiocarboxylate (Hmmeecd) and its propyl homologue (Hmmpcd)¹⁹ containing N₄S donor sites (Scheme 1) capable of offering sufficient structural non-rigidity have been employed. One interesting feature of this type of molecule as previously established^{13,20,21} is the presence of extended electron delocalization due to which the C=S bond behaves predominantly like thiolate as confirmed by X-ray crystallography.^{13,21} Thus, a combination of thiol like sulfur and pendent pyrazolyl groups in these ligands offer a donor environment close to the mononuclear active sites of blue copper proteins.^{22–25} This has motivated us also to investigate the corresponding Cu(II) complexes with these ligands. Herein we report the synthesis, structure, and spectroscopic and electrochemical properties of zinc(II) and copper(II) complexes of these ligands.

- (13) Kumar, S. B.; Bhattacharyya, S.; Dutta, S. K.; Tiekink, E. R. T.; Chaudhury, M. J. *Chem. Soc., Dalton Trans.* **1995**, 2619.
- (14) Dutta, S. K.; Kumar, S. B.; Bhattacharyya, S.; Chaudhury, M. J. *Chem. Soc., Dalton Trans.* **1994**, 97.
- (15) Kumar, S. B.; Chaudhury, M. J. *Chem. Soc., Dalton Trans.* **1992**, 3439.
- (16) Kumar, S. B.; Chaudhury, M. J. *Chem. Soc., Dalton Trans.* **1992**, 269.
- (17) Chaudhury, M. *Inorg. Chem.* **1985**, *24*, 3011.
- (18) Chaudhury, M. *Inorg. Chem.* **1984**, *23*, 4434.
- (19) Abbreviation used: Hmmeecd, methyl ((2-(β-bis((3,5-dimethylpyrazol-1-yl)methyl)amino)ethyl)amino)cyclopent-1-ene-1-dithiocarboxylate; Hmmpcd, methyl ((2-(β-bis((3,5-dimethylpyrazol-1-yl)methyl)amino)propyl)amino)cyclopent-1-ene-1-dithiocarboxylate; dien, diethylenetriamine; bipyam; di-2-pyridylamine; tbp; trigonal bipyramid.
- (20) (a) Mondal, S. K.; Paul, P.; Roy, R.; Nag, K. *Transition. Met. Chem. (Weinheim, Ger.)* **1984**, *9*, 247. (b) Roy, R.; Chaudhury, M.; Mondal, S. K.; Nag, K. *J. Chem. Soc., Dalton Trans.* **1984**, 1681 and references therein.
- (21) (a) Bereman, R. D.; Churchill, M. R.; Shields, G. *Inorg. Chem.* **1979**, *18*, 3117. (b) Martin, E. M.; Bereman, R. D.; Singh, P. *Inorg. Chem.* **1991**, *30*, 957.
- (22) Sorrel, T. N. *Tetrahedron* **1989**, *45*, 3.
- (23) (a) Karlin, K. D.; Gultneh, Y. *Prog. Inorg. Chem.* **1987**, *35*, 219. (b) *Copper Coordination Chemistry: Biochemical and Inorganic Perspectives*; Karlin, K. D.; Zubieta, J. Eds.; Adenine: Guilderland, NY, 1983.
- (24) (a) Kitajima, N. *Adv. Inorg. Chem.* **1992**, *39*, 1. (b) Kitajima, N.; Fujisawa, K.; Moro-oka, Y. *J. Am. Chem. Soc.* **1990**, *112*, 3210.
- (25) Thompson, J. S.; Marks, T. J.; Ibers, J. A. *J. Am. Chem. Soc.* **1979**, *101*, 4180.

Experimental Section

All reactions were carried out under dry nitrogen atmosphere unless otherwise stated. Methyl 2-(β-(aminoalkyl)amino)cyclopent-1-ene-1-dithiocarboxylate,²⁶ 1-(hydroxymethyl)-3,5-dimethylpyrazole,²⁷ and [Cu(CH₃CN)₄]ClO₄²⁸ were prepared following reported methods. Cyclopentanone (E. Merck), ethylenediamine (BDH), hydrazine hydrate (SD Chemicals), 1,2-diaminopropane, and acetylacetone (Fluka) were freshly distilled before use. Solvents were analytical grade, dried from appropriate reagents,²⁹ and distilled under nitrogen prior to their use. All other chemicals were reagent grade and used as received.

Syntheses. Ligands. The pentadentate ligands **Hmmeecd** and **Hmmpcd** were prepared following a published procedure.²⁷

Hmmeecd. A solution of methyl 2-((β-aminoethyl)amino)cyclopent-1-enedithiocarboxylate²⁶ (2.2 g, 10 mmol) in 1,2-dichloroethane (50 mL) was added to a solid sample of 1-(hydroxymethyl)-3,5-dimethylpyrazole²⁷ (2.52 g, 20 mmol), taken in a 100-mL round-bottomed flask. The yellow colored mixture was stirred at room temperature for 24 h and filtered. From the filtrate, solvent was removed under vacuum to a dense yellow semisolid mass, which on trituration afforded solid lumps. The product was recrystallized from petroleum ether (60–80 °C) as golden yellow crystals. Yield: 3.7 g (86%). Mp: 106–107 °C. Anal. Calcd for C₂₁H₃₂N₆S₂: C, 58.33; H, 7.40; N, 19.44. Found: C, 57.9; H, 7.7; N, 19.5. IR (KBr pellet), cm⁻¹: ν(N–H···S) 2920 m, ν(C=C) + ν(C=N)/pyrazole ring, 1595 vs; ν(C=N) + ν(C=C), 1490 s. Absorption spectrum (CH₃CN), λ_{max}/nm (ε_M/mol⁻¹ cm²): 395 (24 450); 312 (10 600); 216 (19 450). ¹H NMR (300 MHz, CD₂Cl₂, 25 °C), δ/ppm: 11.18 (s, 1H, NH···S), 5.82 (s, 2H, pz rings), 4.95 (s, 4H, CH₂), 3.12 (q, 6.2 Hz, 2H, CH₂), 2.97 (t, 6.2 Hz, 2H, CH₂), 2.75 (t, 7.0 Hz, 2H, CH₂/cyclopentene ring), 2.53 (m, 5H, SCH₃ and CH₂/cyclopentene ring), 2.21 (s, 6H, CH₃/pz ring), 2.13 (s, 6H, CH₃/pz ring), 1.81 (q, 7.4 Hz, 2H, CH₂/cyclopentene ring).

Hmmpcd. The procedure was similar to that described for **Hmmeecd** except that methyl 2-((β-aminopropyl)amino)cyclopent-1-enedithiocarboxylate²⁶ was used as a starting material (yield, 82%); mp 123–124 °C. Anal. Calcd for C₂₂H₃₄N₆S₂: C, 59.19; H, 7.40; N, 18.83. Found: C, 59.2; H, 7.7; N, 18.9. IR (KBr pellet), cm⁻¹: ν(N–H···S) 2920 m; ν(C=C) + ν(C=N)/pyrazole ring, 1590 vs; ν(C=N) + ν(C=C), 1470 s. Absorption spectrum (CH₃CN), λ_{max}/nm (ε_M/mol⁻¹ cm²): 397 (24 200); 311 (10 700); 216 (19 600). ¹H NMR (300 MHz, CD₂Cl₂, 25 °C), δ/ppm: 11.16 (s, 1H, NH···S), 5.79 (s, 2H, pz rings), 5.04 (s, 4H, CH₂), 3.01 (m, 2H, CH₂), 3.28 (m, 1H, CH), 2.74 (m, 2H, CH₂/cyclopentene ring), 2.54 (s) + 2.45 (m) (5H, SCH₃ and CH₂/cyclopentene ring), 2.20 (s, 6H, CH₃/pz ring), 2.16 (s, 6H, CH₃/pz ring), 1.81 (m, 2H, CH₂/cyclopentene ring), 1.04 (s) + 1.02 (s) (3H, CH₃).

Complexes. Safety Note! Caution! Perchlorate salts of metal complexes are potentially explosive when shocked or heated.³⁰ The following complexes were isolated in small amounts as their perchlorates and handled with sufficient care.

[Zn(mmeecd)]ClO₄, 1a. To a stirred methanolic solution (15 mL) of **Hmmeecd** (0.43 g, 1 mmol) was added dropwise an equimolar amount of Zn(ClO₄)₂·6H₂O also in methanol (15 mL), and precipitation of a yellow solid began. After the mixture had been stirred for 1 h, the yellow powder was collected by filtration, washed with diethyl ether, and dried under vacuum. The compound was recrystallized from acetone/hexane. Yield: 0.38 g (63%). Anal. Calcd for ZnC₂₁H₃₁N₆S₂ClO₄: C, 42.29; H, 5.20; N, 14.09. Found: C, 41.8, H, 5.3; N, 13.6. IR (KBr pellet), cm⁻¹: ν(C=C), 1570 s, ν(C=N)/pyrazole ring, 1545 s; ν(C=N) + ν(C=C), 1465 vs; ν_{as}(Cl–O), 1095 vs; δ(O–Cl–O), 625 s. Λ_M (CH₃CN): 106 Ω⁻¹ cm² mol⁻¹.

[Zn(mmpcd)]ClO₄, 1b, was obtained in 70% yield following the same procedure as for **1a** but using **Hmmpcd** as the ligand. Anal. Calcd for ZnC₂₂H₃₃N₆S₂ClO₄: C, 43.29; H, 5.41; N, 13.77. Found: C, 43.5; H, 5.7; N, 13.7. IR (KBr pellet), cm⁻¹: ν(C=C), 1565 s;

- (26) Roy, R.; Mondal, S. K.; Nag, K. *J. Chem. Soc., Dalton Trans.* **1983**, 1935.
- (27) Driessen, W. L. *Recl. Trav. Chim. Pays-Bas* **1982**, *101*, 441.
- (28) Hemmerich, P.; Sigwart, C. *Experientia* **1963**, *19*, 488.
- (29) Perrin, D. D.; Armarego, W. L. F.; Perrin, D. R. *Purification of Laboratory Chemicals*, 2nd ed.; Pergamon: Oxford, England, 1980.
- (30) Robinson, W. R. *J. Chem. Educ.* **1985**, *62*, 1001.

$\nu(\text{C}=\text{N})/\text{pyrazole ring}$, 1550 s; $\nu(\text{C}=\text{N}) + \nu(\text{C}=\text{C})$, 1470 vs; $\nu_{\text{as}}(\text{Cl}-\text{O})$, 1095 vs; $\delta(\text{O}-\text{Cl}-\text{O})$, 630 s. $\Lambda_{\text{M}}(\text{CH}_3\text{CN})$: 118 $\Omega^{-1} \text{ cm}^2 \text{ mol}^{-1}$.

[Cu(mmeed)]ClO₄, 2a. To a stirred acetonitrile solution (15 mL) of $[\text{Cu}(\text{CH}_3\text{CN})_4]\text{ClO}_4$ (0.33 g, 1 mmol) was added slowly a solution of **Hmmeed** (0.43 g, 1 mmol) in the same solvent to give a red brown color. The solution was stirred at room temperature for 2 h and filtered. The filtrate volume was reduced to ca. 5 mL by rotaevaporation and then opened to air for 2 h. During this period the initial red brown solution turned to olive green. Storage at 0 °C overnight yielded dark green crystalline solids. These were collected by filtration, washed with diethyl ether, dried in vacuo, and finally recrystallized from $\text{CH}_3\text{CN}/\text{Et}_2\text{O}$. Yield: 0.32 g (54%). Anal. Calcd for $\text{CuC}_{21}\text{H}_{31}\text{N}_6\text{S}_2\text{ClO}_4$: C, 42.42; H, 5.21; N, 14.14. Found: C, 43.4; H, 5.5; N, 14.4. IR (KBr pellet), cm^{-1} : $\nu(\text{C}=\text{C})$, 1570 s; $\nu(\text{C}=\text{N})/\text{pyrazole ring}$, 1540 s; $\nu(\text{C}=\text{N}) + \nu(\text{C}=\text{C})$, 1465 vs; $\nu_{\text{as}}(\text{Cl}-\text{O})$, 1090 vs; $\delta(\text{O}-\text{Cl}-\text{O})$, 620 s. $\Lambda_{\text{M}}(\text{CH}_3\text{OH})$: 89 $\Omega^{-1} \text{ cm}^2 \text{ mol}^{-1}$. μ_{eff} : 1.82 μ_{B} .

[Cu(mmpcd)]ClO₄, 2b. This compound was obtained in 55% yield by an identical procedure as reported above for **2a** using **Hmmpcd** as the ligand. Anal. Calcd for $\text{CuC}_{22}\text{H}_{33}\text{N}_6\text{S}_2\text{ClO}_4$: C, 43.42; H, 5.42; N, 13.81. Found: C, 45.1; H, 5.5; N, 15.1. IR (KBr pellet), cm^{-1} : $\nu(\text{C}=\text{C})$, 1570 s; $\nu(\text{C}=\text{N})/\text{pyrazole ring}$, 1540 s; $\nu(\text{C}=\text{N}) + \nu(\text{C}=\text{C})$, 1460 vs; $\nu_{\text{as}}(\text{Cl}-\text{O})$, 1085 vs; $\delta(\text{O}-\text{Cl}-\text{O})$, 620 s. $\Lambda_{\text{M}}(\text{CH}_3\text{OH})$: 95 $\Omega^{-1} \text{ cm}^2 \text{ mol}^{-1}$. μ_{eff} : 1.84 μ_{B} .

[(Cu,Zn)(mmpcd)]ClO₄. Complexes **1b** (100 mg, 0.16 mmol) and **2b** (7.5 mg, 0.012 mmol) were dissolved together in acetone (10 mL). To this solution was added *n*-hexane (2 mL) drop by drop under stirring, and the mixture was stored in a freezer (0 °C) overnight to get a pale green solid. The product was collected by filtration, washed with *n*-hexane, dried, and finally recrystallized from acetone/*n*-hexane. Yield: 88 mg. The copper content (ca. 5.0 mol %) was determined spectrophotometrically by measuring the optical density of the solution in acetonitrile at 608 nm.

Physical Measurements. Details of IR, UV/visible, and room temperature magnetic measurements have been described elsewhere.¹⁴ Electronic spectra with the solid samples were determined using a Hitachi Model U-3410 spectrophotometer. Solution electrical conductivities were measured with a Systronics Model 304 bridge. The ¹H NMR spectra were recorded on a Bruker AC 300 apparatus. The X-band EPR spectra in the solution (dichloromethane/toluene 1:10 v/v) at room temperature as well as in the frozen state (77 K) were recorded on a Varian E-line Century Series Instrument equipped with Varian E-102 microwave bridge and Oxford Instrument ITC-4 temperature controller. Electrochemical measurements were carried out in acetonitrile containing 0.1 M Bu₄NBF₄ using a three electrode configuration (glassy-carbon working electrode, platinum-wire counter electrode, and Ag/AgNO₃ as reference) and a PAR 362 scanning potentiostat. The ferrocene/ferrocenium (Fc/Fc⁺) couple was used as internal standard.³¹ Elemental analyses were performed with a Perkin-Elmer 240C elemental analyzer by the microanalytical laboratory of this department at the Indian Association for the Cultivation of Science.

X-ray Crystallography. Diffraction quality crystals of **1b** were grown at room temperature by slow diffusion of *n*-hexane into an acetone solution of the complex. Crystals of **2b** were obtained following identical procedure from $\text{CH}_3\text{CN}/\text{Et}_2\text{O}$. Intensity data for a pale yellow crystal of **1b** (0.11 × 0.19 × 0.40 mm) and a dark blue crystal of **2b** (0.07 × 0.21 × 0.47 mm) were measured at room temperature on a Rigaku AFC 6R diffractometer fitted with graphite monochromatized Mo K α radiation, $\lambda = 0.71073 \text{ \AA}$. The $\omega:2\theta$ scan technique was employed to measure data in each case upto a maximum Bragg angle θ of 25°. No decomposition of the crystals occurred during the data collections. Lorentz and polarization corrections³² were applied as was an empirical absorption correction³³ (transmission factors were in the range 0.922–1.029 for **1b** and 0.898–1.200 for **2b**). Relevant crystallographic data are given in Table 1.

For compound **1b**, a total of 5057 (5265 for **2b**) reflections were scanned, and of these, 3549 (2710 for **2b**) unique reflections which satisfied the $I \geq 3.0\sigma(I)$ criterion were used for the structure solution

Table 1. Summary of Crystallographic Data

	1b	2b
formula	C ₂₂ H ₃₃ ClN ₆ O ₄ S ₂ Zn	C ₂₂ H ₃₃ ClCuN ₆ O ₄ S ₂
fw	610.5	608.6
space group	<i>P</i> 1̄ (No. 2)	<i>P</i> 2 ₁ / <i>n</i> (No. 14)
<i>a</i> , Å	9.900(3)	12.859(6)
<i>b</i> , Å	15.379(5)	12.642(3)
<i>c</i> , Å	8.858(2)	16.503(2)
α , deg	99.93(2)	90
β , deg	93.62(2)	102.67(2)
γ , deg	100.38(2)	90
<i>V</i> , Å ³	1300.5(7)	2617(1)
<i>Z</i>	2	4
<i>T</i> , °C	25	25
$\lambda(\text{Mo K}\alpha)$, Å	0.71073	0.71073
ρ_{calcd} , g cm ⁻³	1.551	1.537
μ , cm ⁻¹	12.49	11.37
<i>R</i> ^a (<i>R</i> _w ^b)	0.042 (0.047)	0.049 (0.056)

$$^a R = \sum(|F_o| - |F_c|) / \sum|F_o|. \quad ^b R_w = [\sum w(|F_o| - |F_c|)^2 / \sum w|F_o|^2]^{1/2}.$$

and refinement. The structures were solved by direct methods³⁴ and refined by a full-matrix least-squares procedure based on *F*.³² Scattering factors for all atoms were those incorporated in the teXsan program.³² Non-H atoms were refined with anisotropic thermal parameters and H atoms were included in the models in their calculated positions (C–H 0.97 Å). In the refinement of **2b** some disorder was noted in the C(3)–C(7) ring as evidenced by relatively high thermal motion associated with the C(7) atom in particular; no evidence was found for multiple sites for this atom. The refinements were continued until convergence employing sigma weights that yielded the final *R* of 0.042 (*R*_w = 0.047) for **1b** and 0.049 (*R*_w = 0.056) for **2b**. The largest peak heights from the final difference Fourier map were 0.46 and 0.57 e/Å³ for **1b** and **2b**, respectively. Molecular structures were drawn with ORTEP³⁵ at 25% probability ellipsoids. The teXsan³² package, installed on an Iris Indigo workstation, was employed for all calculations.

Results and Discussion

Synthesis. Two new pentadentate ligands **Hmmeed** and **Hmmpcd** both having N₄S donor atoms set were synthesized following a route illustrated in Scheme 1 which involve condensation reaction between the precursor amines²⁶ and 1-(hydroxymethyl)-3,5-dimethylpyrazole in dichloroethane. Some complexation reactions of these ligands were examined. The zinc(II) complexes $[\text{Zn}(\text{mmeed})]\text{ClO}_4$ (**1a**) and $[\text{Zn}(\text{mmpcd})]\text{ClO}_4$ (**1b**) were readily obtained as yellow solids by mixing equimolar amounts of zinc perchlorate hexahydrate with the free ligands in methanol. The perchlorate salts were isolated and recrystallized from acetone/hexane mixture. An identical procedure with copper(II) perchlorate hexahydrate used instead of zinc(II) perchlorate, yielded brown intractable solid of unknown composition possibly due to reduction of copper(II) by the ligands (*vide infra*). This had prompted us to adopt an alternative strategy in which $[\text{Cu}^+(\text{CH}_3\text{CN})_4]\text{ClO}_4$ was allowed to react with stoichiometric amount of the ligand in CH_3CN under strict anaerobic condition. The red brown solution obtained at this stage on exposure to air transformed into olive green color from which dark green copper(II) complexes (**2a**, **2b**) were isolated. Molar conductivities of the zinc(II) complexes in acetonitrile (106, **1a** and 118, **1b**) and the copper(II) complexes in methanol (89, **2a** and 95 $\Omega^{-1} \text{ cm}^2 \text{ mol}^{-1}$, **2b**) are in accord with 1:1 electrolytic behavior.³⁶

IR spectra of the free ligands show a very strong band due to combination of cyclopentene $\nu(\text{C}=\text{C})$ and pyrazole

(31) Gagne, R. R.; Koval, C. A.; Lisensky, G. C. *Inorg. Chem.* **1980**, *19*, 3854.

(32) teXsan: Structure Analysis Software. Molecular Structure Corporation, Texas, U.S.A.

(33) Walker, N.; Stuart, D. *Acta Crystallogr.* **1983**, *A39*, 158.

(34) Sheldrick, G. M. SHELSX 86 Program for the Automatic Solution of Crystal Structure. University of Göttingen, Germany, 1986.

(35) Johnson, C. K. ORTEP. Report ORNL-5138: Oak Ridge National Laboratory: Oak Ridge, TN, 1976.

(36) Geary, W. J. *Coord. Chem. Rev.* **1971**, *7*, 81.

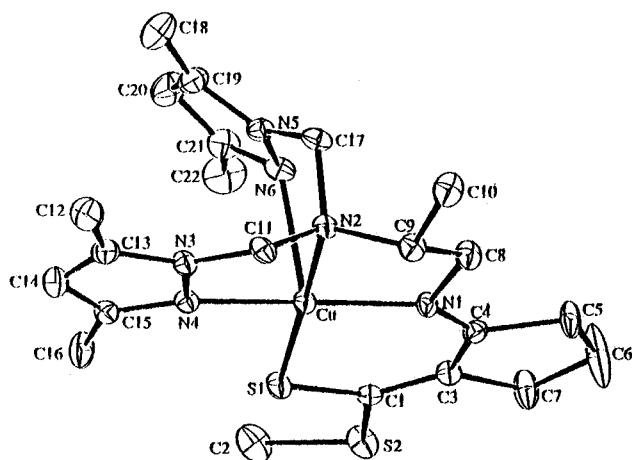


Figure 1. ORTEP plot of the complex cation in $[\text{Cu}(\text{mmpcd})]\text{ClO}_4$ (**2b**) giving the crystallographic atom-numbering scheme. 25% probability ellipsoids are shown.

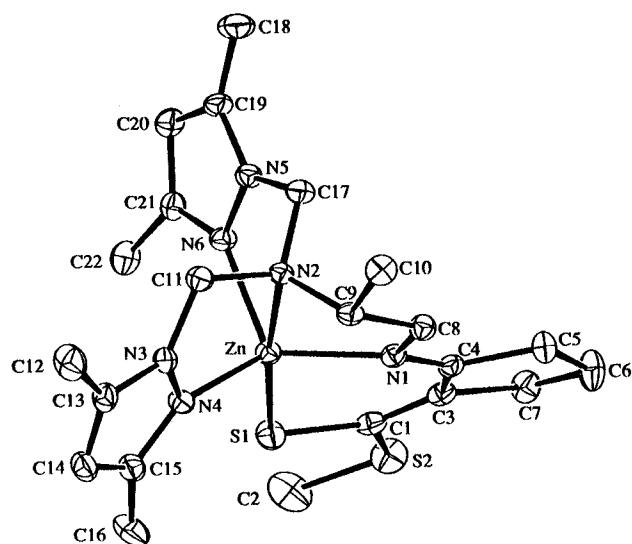


Figure 2. Structure of $[\text{Zn}(\text{mmpcd})]^+$ as the ClO_4^- salt **1b**, showing 25% probability ellipsoids and the atom-labeling scheme.

$\nu(\text{C}\equiv\text{N})$ vibrations at 1590 cm^{-1} . This band splits into two components of almost equal intensities in the complexes appearing at 1570 and 1550 cm^{-1} , indicative of coordination of the pyrazolyl groups to the metal. The complexes also have two strong bands, one broad feature centering around 1095 cm^{-1} due to $\nu_{\text{as}}(\text{Cl}-\text{O})$ and the other having a sharp feature at 620 cm^{-1} due to $\delta(\text{O}-\text{Cl}-\text{O})$, confirming the presence of ionic perchlorate³⁷ in these molecules.

Description of Crystal Structures. The molecular structures of the cations in **2b** and **1b** along with the atom-labeling schemes are shown in Figures 1 and 2, respectively. Selected bond distances and angles pertaining to the metal coordination spheres for both structures are given in Table 2. There are no significant interionic contacts in the crystal structure of **2b** with the closest non-H contact of $3.283(6)\text{ \AA}$ occurring between the S(2) and N(6)' atoms (symmetry operation: $0.5 - x, -0.5 + y, 0.5 - z$). The ligand is pentadentate, utilizing all potential donor atoms in coordination. In the absence of $\text{Cu}\cdots\text{perchlorate}$ interactions, the Cu atom is thus five-coordinate and exists in a geometry based on a square pyramid. The S(1), N(1), N(2), and N(4) atoms define the basal plane and lie $+0.014(2)$, $-0.106(6)$, $+0.111(6)$, and $-0.092(6)\text{ \AA}$, respectively, out of the least-

Table 2. Selected Bond Distances (\AA) and Angles (deg) for **1b** and **2b**

	2b	1b
	M = Cu	M = Zn
M-S(1)	2.216(2)	2.294(1)
M-N(1)	1.942(5)	2.013(3)
M-N(2)	2.086(5)	2.345(3)
M-N(4)	2.017(5)	2.024(3)
M-N(6)	2.388(6)	2.043(3)
S(1)-C(1)	1.700(7)	1.706(5)
N(1)-C(4)	1.287(8)	1.280(5)
N(1)-C(8)	1.465(8)	1.457(5)
N(2)-C(9)	1.488(9)	1.454(5)
N(2)-C(11)	1.447(9)	1.434(5)
N(2)-C(17)	1.472(9)	1.443(5)
N(3)-N(4)	1.356(8)	1.350(4)
N(3)-C(11)	1.438(9)	1.447(5)
N(5)-N(6)	1.356(8)	1.354(4)
N(5)-C(17)	1.421(9)	1.446(5)
C(1)-C(3)	1.346(9)	1.354(6)
C(3)-C(4)	1.424(9)	1.430(6)
C(8)-C(9)	1.470(1)	1.505(6)
S(1)-M-N(1)	97.2(2)	97.0(1)
S(1)-M-N(2)	177.2(2)	173.69(9)
S(1)-M-N(4)	96.9(2)	106.8(1)
S(1)-M-N(6)	102.3(1)	110.8(1)
N(1)-M-N(2)	84.7(2)	76.9(1)
N(1)-M-N(4)	161.5(2)	122.0(1)
N(1)-M-N(6)	99.2(2)	114.3(1)
N(2)-M-N(4)	80.8(2)	75.9(1)
N(2)-M-N(6)	79.3(2)	73.4(1)
N(4)-M-N(6)	89.5(2)	105.3(1)
M-S(1)-C(1)	107.5(2)	104.2(1)
M-N(1)-C(4)	129.8(5)	124.0(3)
M-N(1)-C(8)	112.7(4)	117.8(3)
M-N(2)-C(9)	104.1(4)	102.5(2)
M-N(2)-C(11)	106.8(4)	105.3(2)
M-N(2)-C(17)	110.4(4)	105.3(2)
N(4)-N(3)-C(11)	118.2(5)	119.8(3)
M-N(4)-N(3)	111.2(4)	117.3(2)
M-N(4)-C(15)	142.6(5)	137.8(3)
M-N(6)-N(5)	97.2(4)	117.4(2)
M-N(6)-C(21)	131.1(5)	137.4(3)
S(1)-C(1)-C(3)	128.8(5)	129.3(3)
C(1)-C(3)-C(4)	127.9(6)	128.4(4)
N(1)-C(4)-C(3)	126.6(6)	129.1(4)
N(1)-C(8)-C(9)	110.4(6)	112.6(3)
N(2)-C(9)-C(8)	110.0(6)	109.0(3)
N(2)-C(11)-N(3)	107.2(6)	109.3(3)

squares plane through them; the Cu atom lies $0.0981(9)\text{ \AA}$ out of this plane in the direction of N(6) atom, which occupies the apical position. The maximum distortion from the ideal geometry is manifested in the N(1)-Cu-N(4) angle of $161.5(2)^\circ$ which reflects the restricted bite angle of the ligand. The three Cu-N bond distances in the basal plane lie in the relatively narrow range $1.942(5)$ – $2.086(5)\text{ \AA}$ with the apical Cu-N separation being significantly longer at $2.388(6)\text{ \AA}$. Deprotonation of the ligand is at the N(1) atom which forms the shortest Cu-N contact of $1.942(5)\text{ \AA}$. The C(1)-S(1) distance of $1.700(7)\text{ \AA}$ indicates that this group has significant thiol-like character owing to the delocalization of π -electron density over the Cu, S(1), C(1), C(3), C(4), and N(1) atoms, which define an essentially planar six-membered ring; the Cu/S(1)/C(1)/C(3), Cu/N(1)/C(4)/C(3) and S(1)/C(1)/C(3)/C(4) torsion angles are $+13.8(7)$, $-5(1)$ and $-5(1)^\circ$, respectively. The C(1)-C(3) [$1.346(9)\text{ \AA}$], C(3)-C(4) [$1.424(9)\text{ \AA}$], and N(1)-C(4) [$1.287(8)\text{ \AA}$] separations corroborate this conclusion. The three five-membered rings are puckered owing to the presence of sp^3 C centers.

In **1b** (Figure 2) the crystal lattice comprises essentially discrete entities with the closest non-hydrogen contact of

(37) Nakamoto, K. *Infrared and Raman Spectra of Inorganic and Coordination Compounds*, 3rd ed.; Wiley-Interscience: New York, 1978.

3.161(5) Å occurring between the perchlorate O(4) and N(3)'' atoms (symmetry operation: $1 - x, 1 - y, 1 - z$). The ligand is again pentadentate, however, in **1b** defines a distorted trigonal bipyramidal geometry about the Zn atom, highlighting the flexibility of the ligand. In this description the trigonal plane is defined by the N(1), N(4), and N(6) atoms with the Zn atom 0.5079(5) Å out of this plane in the direction of the S(1) atom. The axial sites are occupied by the S(1) and N(2) atoms such that the S(1)–Zn–N(2) angle is 173.69 (9)°. The axial–Zn–equatorial S(1)–Zn–N angles are greater than 90°, i.e. 97.0(1)–110.8(1)°, and the N(2)–Zn–N angles are acute, i.e. N(2)–Zn–N = 73.4(1)–76.9(1)°, reflecting the significant distance the Zn atom lies out of the equatorial plane. The Zn/S(1)/C(1)/C(3), Zn/N(1)/C(4)/C(3), and S(1)/C(1)/C(3)/C(4) torsion angles of –17.4(4), +14.4(6), and –1.8(7)°, respectively, indicate some puckering in the Zn, S(1), C(1), C(3), C(4), and N(1) six-membered ring, at least more so than that observed in **2b**. There are some substantial changes in some of the metal–ligand separations in the two structures (Table 2), which reflect the different coordination geometries.

Whereas the M–N(4) bond distances are equal within experimental error [Cu–N(4), 2.017(5) Å; Zn–N(4), 2.024(3) Å], the Zn–S(1), Zn–N(1), and Zn–N(2) distances are approximately 0.08, 0.07, and 0.26 Å longer, respectively, than the corresponding distances in **2b**. By contrast, the Zn–N(6) separation is approximately 0.35 Å shorter than the Cu–N(6) distance. In particular, the large differences in the M–N(2) and M–N(6) separations reflect the interchanging of the atoms between axial/apical and equatorial positions in the two structures. The major change in the angles subtended at the metal center in two structures involves N(1)–M–N(4), which expands from 122.0(1)° in **1b** to 161.5(2)° in **2b**, reflecting the change in the mode of coordination of the ligand. The geometric parameters defining the ligands are in essential agreement in the two structures with a few notable exceptions associated with the N(2) and N(6) atoms.

Allowing for the observation that the derived estimated standard deviations for the light atom parameters are relatively high it is still possible to discern some definite trends in the two structures. Notably the N(2)–C bond distances in **1b** are shorter (Table 2) than the corresponding distances in **2b** which correlates with the weaker Zn–N(2) interaction. It is also significant that the N(3)–C(11), N(5)–C(17), and C(8)–C(9) bond distances are longer in **1b** compared to **2b**. The bond distances associated with the N(6) atom are less susceptible to change owing to the high degree of delocalization of π -electron density in the Me₂pz rings, however, there are significant differences in the bond angles about the N(6) atom where the Zn–N(6)–N(5) and Zn–N(6)–C(21) angles in **1b** have expanded by approximately 20 and 6°, respectively.

¹H NMR Spectra. The proton NMR spectra of **Hmmedc** and **Hmmpcd** and corresponding zinc(II) complexes **1a** and **1b** were recorded in CD₂Cl₂ at 300 MHz. The free ligands exhibit a broad resonance due to the N–H⋯S functionality at ca. 11.18 ppm, which is missing in the complexes. More importantly while the methylene protons H-11 and H-17 of the pyrazolyl arms appear as a singlet at ca. 5.0 ppm in the free ligands, they become anisochronous in the complexes. For example, in **1a** these methylene protons are observed as a AB quartet with $\delta_A = 5.16$ ppm and $\delta_B = 4.94$ ppm ($J_{AB} = 11.96$ Hz). On the other hand, due to the presence of a chiral center in **1b** at C-9, inequivalent diastereotopic proton signals are obtained as two AB quartets at 5.45, 5.25, 4.82, and 4.43 ppm ($J_{AB} = 12.45$ Hz and $J_{A'B'} = 11.80$ Hz) for these methylene protons (Figure 3). This is also evident from the fact that the singlet due to pyrazole

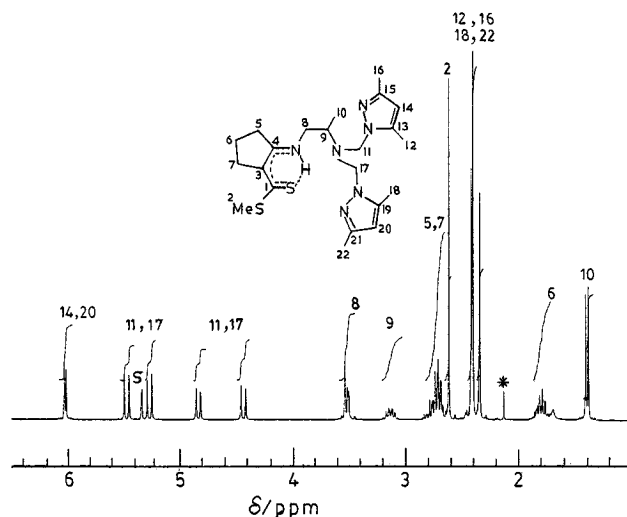


Figure 3. ¹H NMR spectrum of [Zn(mmpcd)]ClO₄ (**1b**) in CD₂Cl₂. The peak marked with an asterisk denotes impurity.

Table 3. Magnetic Moment and EPR Data for the Copper(II) Complexes

com- pound	μ_{eff}^d	$\langle g \rangle^b$	$10^4 \langle A \rangle /$ $\text{cm}^{-1}{}^b$	g_{\parallel} (g_3)	g_{\perp} (g_1, g_2)	$10^4 A_{\parallel}$ ($10^4 A_3$) / cm^{-1}	$10^4 A_{\perp}$ ($10^4 A_1$) / cm^{-1}
2a	1.82	2.140	138	2.151 ^a	2.010 ^a	156 ^c	
				2.204 ^c	2.106 ^c		
2b	1.84	2.131	134	2.152 ^a	1.995 ^a	154 ^c	
				2.202 ^c	2.102 ^c		
				(2.188) ^d	(2.139) ^d		

^a Measured at room temperature with polycrystalline sample. ^b From room temperature spectra in CH₂Cl₂/toluene (1:10 v/v) solution. ^c From frozen solution (78 K) spectra. ^d From doped (5% Cu/Zn) sample.

ring protons H-14 and H-20 in **Hmmpcd** (5.79 ppm) appears as a pair of singlets (6.00 and 6.02 ppm) in **1b**. By contrast no such twinning occurs in the case of **1a** (6.01 ppm). Detailed assignments of the NMR spectra are given in Table S(11) (see Supporting Information).

Magnetic Susceptibility and EPR Spectra. Magnetic moments and EPR parameters of the copper(II) complexes (**2a**, **2b**) are summarized in Table 3. At room temperature, powdered polycrystalline samples of complexes have magnetic moments 1.82 (**2a**) and 1.84 μ_B (**2b**) somewhat higher than the spin-only value. Such divergence is not quite uncommon in mononuclear Cu(II) complexes due to mixing-in of some orbital angular momentum from the closely lying excited states via spin–orbit coupling.³⁸

The X-band EPR spectra at room temperature (298 K) of the copper(II) complexes in powdered polycrystalline state revealed axial symmetry with $g_{\parallel} = 2.15$ and $g_{\perp} = 1.99$ indicating an apically elongated tetragonal environment for copper(II) ion with a $d_{x^2-y^2}$ ground state.³⁹ In solution (dichloromethane/toluene, 1:10 v/v) on the other hand the compounds exhibited typical four-line splitting patterns at room temperature with $\langle g \rangle = 2.13$ and $\langle A \rangle = 134 \times 10^{-4} \text{ cm}^{-1}$ due to interaction of the unpaired electron with the nuclear spin of the copper nucleus (^{63,65}Cu; $I = 3/2$), which in the frozen glass (78 K) displayed axial anisotropy (Figure 4a)⁴⁰ with some rhombical distortions.⁴¹ The observed features (Table 3) $g_{\parallel} > g_{\perp}$ with $A_{\parallel} = 154 \times 10^{-4}$

(38) Figgis, B. N.; Lewis, J. In *Modern Coordination Chemistry: Principles and Methods*; Lewis, J., Wilkins, R. G. Eds.; Interscience: New York, 1960; Chapter 6, p 400.

(39) (a) Hathaway, B. J.; Billing, D. E. *Coord. Chem. Rev.* **1970**, *5*, 143. (b) Elliot, H.; Hathaway, B. J.; Slade, R. C. *J. Chem. Soc. A* **1966**, 1443.

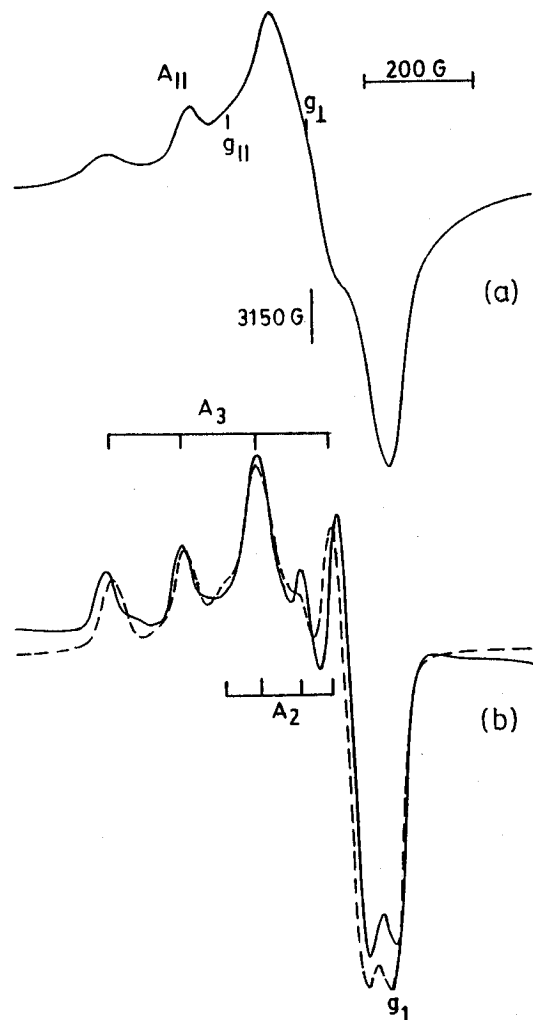


Figure 4. (a) Frozen-solution X-band EPR spectrum (78 K) of $[\text{Cu}(\text{mmpcd})]\text{ClO}_4$ (**2b**) in $\text{CH}_2\text{Cl}_2/\text{toluene}$ (1:10 v/v): frequency, 9.245 GHz; gain, 4×10^3 . (b) Polycrystalline powder EPR spectra at 298 K (---) and 78 K (—) of $[\text{Cu}(\text{mmpcd})]\text{ClO}_4$ (**2b**) doped (5%) into $[\text{Zn}(\text{mmpcd})]\text{ClO}_4$ (**1b**) complex: frequency, 9.11 GHz; gain, 2.5×10^2 (298 K) and 1.25×10^2 (78 K).

cm^{-1} are diagnostic of a pseudotetragonal site symmetry for the copper(II) complexes.⁴² When doped (5%) into its zinc counterpart (**1b**) with tbp structure (*vide supra*), the spectrum of **2b** in polycrystalline state is typically rhombic in nature. As shown in Figure 4b the spectrum clearly revealed nuclear hyperfine splittings of the higher g components $g_3 = 2.19$ ($A_3 = 143 \times 10^{-4} \text{ cm}^{-1}$) and $g_2 = 2.14$ ($A_2 = 67.5 \times 10^{-4} \text{ cm}^{-1}$) with an unresolved feature for the lowest g tensor ($g_1 = 1.99$). All these features remained practically unchanged down to liquid nitrogen temperature. Almost a similar rhombic pattern has been reported for a Cu(II) compound with tbp structure in a comparable N_4S donor environment.⁴³ The EPR spectrum of 1% copper-doped $[\text{Zn}(\text{dien})(\text{bipyam})](\text{NO}_3)_2$ has almost a similar rhombic feature where both host and guest species are nearly isomorphous, having distorted tbp structures.^{7f} Spectra of the doped sample (5 mol % of **2b** doped in **1b**) thus provide evidence in favor of enough plasticity in the copper coordination

Table 4. Summary of Electronic Spectral Data in Solution

complex	solvent	$\lambda_{\text{max}}/\text{nm}$ ($\epsilon_{\text{max}}/\text{mol}^{-1} \text{ cm}^2$)
1a	CH_3CN	391 (9500), 375 (11700), 285 (7550), 221 (14200)
1b	CH_3CN	391 (9300), 375 (11400), 285 (7150), 223 (11900)
2a	CH_3CN	608 (290), 391 (7200), 354 (16850), 292 (13000)
	CH_2Cl_2	607 (314), 396 (5200), 358 (16000), 297 (11500)
	CH_3OH	603 (243), 392 (6500), 354 (15800), 293 (11900)
	DMSO	598 (214), 391 (6700), 353 (15000), 293 (11200)
2b	CH_3CN	608 (250), 391 (6000), 354 (14800), 292 (11150)
	DMSO	599 (200), 391 (5350), 354 (13900), 293 (10200)

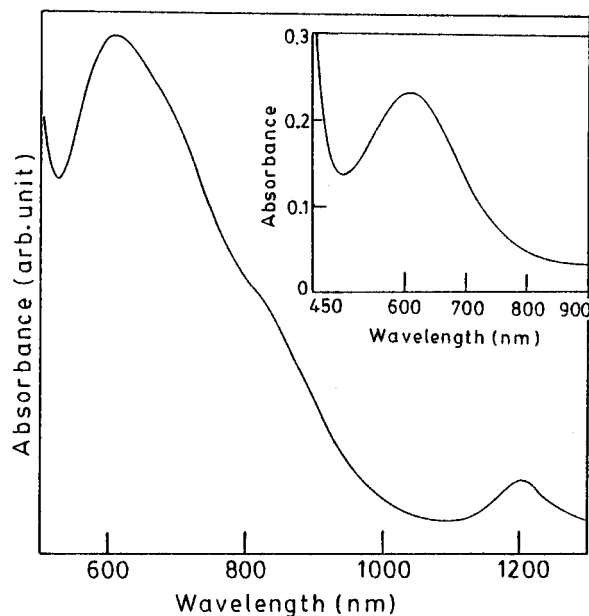


Figure 5. Absorption spectrum of powdered, polycrystalline sample of $[(\text{Cu,Zn})(\text{mmpcd})]\text{ClO}_4$ in a Nujol mull. The inset shows the spectrum of $[\text{Cu}(\text{mmpcd})]\text{ClO}_4$ (**2b**) in acetonitrile.

sphere of **2b** so much so that it can closely imitate the lattice structure of its host in acquiring at least a distorted trigonal geometry.

Electronic Spectra. Electronic spectra of the complexes are summarized in Table 4. The zinc(II) complexes (**1a**, **1b**) in CH_3CN display multiple intense absorptions in the UV region that we assume result from metal–ligand charge-transfer and ligand internal transitions. In the UV region (in CH_3CN) copper(II) complexes (**2a**, **2b**) also have similar absorption features of which the lowest energy band at 391 nm (ϵ , 7200, **2a**; 6000 $\text{mol}^{-1} \text{ cm}^2$, **2b**), we suggest originates from $\text{S}(\pi) \rightarrow \text{Cu}(\text{II})$ charge-transfer on the basis of analogy to similar reported complexes.⁴³ In the visible region spectra of **2a**, **2b** contain a single d–d band (Figure 5, inset) at 608 nm (ϵ , 290 (**2a**), 250 $\text{mol}^{-1} \text{ cm}^2$, (**2b**)) with an additional weak, broad and featureless absorption appearing at *ca.* 1000 nm in the near-IR region (not included in Table 4). Absorption bands with comparable features have been previously assigned to copper(II) complexes having square pyramidal structure with considerable distortions towards tbp.^{42b,44} Spectral properties of **2a** and **2b** were also examined in various solvents which differ in their donor numbers.⁴⁵ As summarized in Table 4 these spectra remained practically unchanged, indicating no significant variation in copper stereochemistry in these solvents.⁴⁶

(40) Spectrum of a representative member **2b** is shown in Figure 4a. Almost identical features are obtained with **2a**.

(41) Lomis, T. J.; Elliot, M. G.; Siddiqui, S.; Moyer, M.; Koepsel, R. P.; Shepherd, R. E. *Inorg. Chem.* **1989**, *28*, 2369.

(42) (a) Chen, S.; Richardson, J. F.; Buchanon, R. M. *Inorg. Chem.* **1994**, *33*, 2376. (b) McLachlan, G. A.; Fallon, G. D.; Martin, R. L.; Spiccia, L. *Inorg. Chem.* **1995**, *34*, 254.

(43) Hughey IV, J. L.; Fawcett, T. G.; Rudich, S. M.; Lalancette, R. A.; Potenza, J. A.; Schugar, H. J. *J. Am. Chem. Soc.* **1979**, *101*, 2617.

(44) (a) Adhikary, B.; Lucas, C. R. *Inorg. Chem.* **1994**, *33*, 1376. (b) Bianchi, A.; Garcia-Espana, E.; Micheloni, M.; Nardi, N.; Vizza, F. *Inorg. Chem.* **1986**, *25*, 4379. (c) Hathaway, B. J. In *Comprehensive Coordination Chemistry*; Wilkinson, G.; Gillard, R. D.; McCleverty, J. A. Eds.; Pergamon Press: Oxford, England, 1987; Vol. 5, p 533.

(45) Guttman, V. *The Donor-Acceptor Approach to Molecular Interactions*; Plenum: New York, 1978.

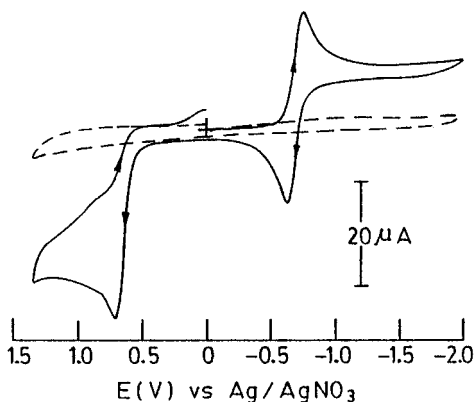
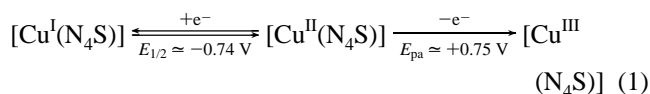


Figure 6. Cyclic voltammogram of [Cu(mmpcd)ClO₄] (**2b**) in acetonitrile with 0.1 M (*n*-Bu)₄NBF₄ as supporting electrolyte and 100 mV/s scan rate using Ag/AgNO₃ reference electrode (the dashed curve indicates the response with the zinc(II) complex **1b** under identical conditions).

As shown in Figure 5, the mull spectrum of the copper(II) complex **2b** doped in the corresponding zinc(II) complex **1b** (5.0 mol %) exhibits a broad absorption maximum at *ca.* 615 nm, a broad shoulder centering around 800 nm, and a relatively narrow absorption feature with the peak at 1215 nm. By contrast, the mull spectrum of **2b** itself shows only a broad shoulder at *ca.* 610 nm. In literature, only a few reports^{47,48} are available with copper(II) complexes having similar near-IR transition. The interpretation of this band as arising from a d–d transition⁴⁸ is not unambiguous because there is much evidence that in this region of spectrum various vibrational overtones can appear.^{49,50} The remaining two bands observed in Figure 5 indicate significant distortion of copper coordination environment towards *tbp* in the doped sample.⁴²

Electrochemistry. The electrochemical behavior of the copper(II) complexes **2a** and **2b** at a glassy carbon electrode in CH₃CN have grossly identical features. The cyclic voltammogram of **2b**, shown in Figure 6 as an example, involves a quasi-reversible reduction ($\Delta E_p \cong 130$ mV, (120 mV for **2a**) and $i_{pc}/i_{pa} \cong 1.0 \pm 0.05$ in the scan rate range 50–500 mV s⁻¹) at -0.74 V (-0.73 V for **2a**) and an irreversible oxidation at +0.75 V (+0.75 V for **2a**) *vs* Ag/AgNO₃. Corresponding zinc(II) complexes are electrode inactive (Figure 6) in this potential range (-2.5 to +1.5 V). The reversible process in the cathodic span thus corresponds to Cu(II)/Cu(I) reduction while the anodic process, a Cu(II)/Cu(III) oxidation. Comparison with the ferrocenium/ferrocene couple as internal standard also suggests these couples to be monoelectronic, forming a three-membered electron-transfer series, given in eq 1, where the net charges on



the species have been omitted for brevity. Exhaustive electrolysis past the reduction process (potential held at -1.0 V *vs* Ag/AgNO₃) established single-electron stoichiometry ($n = 1.0 \pm 0.1$) for this couple. Similar experiments with the oxidation process (working potentials set at *ca.* 0.90 V) however, failed

to provide any meaningful result for the anodic reaction. Nevertheless, the one-electron nature in this case is established from a comparison of current height at E_{pa} to that of the corresponding authentic one-electron current parameter, *viz* E_{pc} , for the reduction couple in Figure 6.

Of particular interest here are the high negative potentials needed to reduce the copper(II) center in **2a** and **2b** compared to many five-coordinated copper(II) complexes involving hard donors, *viz* nitrogen, oxygen, and chlorine, where the Cu(II)/Cu(I) reduction is very much facile ($E_{1/2}$ ranges between -0.3 and +0.22 V *vs* SCE)^{42a,46b,51,52} and Cu(II)/Cu(III) oxidation mostly remains unobserved. Thus presence of sulfur donor(s) in the coordination sphere probably generate conducive electronic environment to stabilize copper in the higher oxidation states as also reported by others.^{53,54}

Concluding Remarks

Zinc(II) and copper(II) complexes of two pentadentate ligands having a N₄S donor assembly amid a sufficiently flexible backbone have been described. The zinc(II) complex **1b** has a trigonal bipyramidal geometry as against a distorted square pyramidal type established for its copper(II) counterpart **2b** by X-ray diffraction analyses. The carbodithioate sulfur in these ligands behaves more like a thiolate and capable of reducing the Cu(II) ion. The Cu(1)–S(1) = 1.700(7) and Cu–S(1) = 2.216(2) Å distances in **2b** are very much in the range observed in similar copper(II)–thiolate complexes.^{43,54} The electronic and EPR spectra in the solid state of the doped copper compound [**2b** (5%) doped in **1b**] confirm sufficient lability in the structure of the copper(II) complex **2b**. The ligand system probably needs a small amount of energy to change its wrapping pattern from one geometry to the other.^{42,44c,55} The influence of the host lattice here suffices to induce structural mimicry in the guest copper(II) complex.⁵⁶

Acknowledgment. We are grateful to the Council of Scientific and Industrial Research, New Delhi (Grant No. 1(1179)/90-EMR-II) for financial support and wish to record our thanks to Professor K. Nag for helpful discussion, to Dr. R. Douthwaite and Professor A. K. Pal for their assistance with EPR and electronic spectral (in solid state) measurements, respectively. Financial assistance received from the Australian Research Council (ARC) for a part of this work is also acknowledged.

Supporting Information Available: Tables of crystallographic details, anisotropic thermal parameters, hydrogen atom parameters, bond lengths and angles, fractional atomic coordinates, and ¹H NMR chemical shifts of the ligands and complexes **1a** and **1b** and packing diagrams for complexes **1b** and **2b** (14 pages). Ordering information is given on any current masthead page. Structure factor amplitudes are available from the authors on request.

IC950594K

- (46) (a) Wu, H.; Lucas, C. R. *Inorg. Chem.* **1993**, *32*, 526. (b) Yao, Y.; Perkovic, M. W.; Rillema, P. D.; Wood, C. *Inorg. Chem.* **1992**, *31*, 3956.
 (47) McKenzie, E. D. *J. Chem. Soc. A* **1970**, 3095.
 (48) Hathaway, B. J.; Dudley, R. J.; Nicholls, P. *J. Chem. Soc. A* **1969**, 1845.
 (49) Bersuker, I. B. *The Jahn-Teller Effect and Vibronic Interactions in Modern Chemistry*; Plenum: New York, 1984.
 (50) We are grateful to one of the reviewers for suggesting this possibility.

- (51) Masood, M. A.; Hodgson, D. J. *Inorg. Chem.* **1993**, *32*, 4839.
 (52) Simmons, M. G.; Merrill, C. L.; Wilson, L. J.; Bottomley, L. A.; Kadish, K. M. *J. Chem. Soc., Dalton Trans.* **1980**, 1827.
 (53) Fortier, D. G.; McAuley, A. *Inorg. Chem.* **1989**, *28*, 655.
 (54) Anderson, O. P.; Perkins, C. M.; Brito, K. K. *Inorg. Chem.* **1983**, *22*, 1267.
 (55) Muettterties, E. L.; Schunn, R. A. *Q. Rev.—Chem. Soc.* **1966**, *20*, 245.
 (56) Sacconi, L.; Ciampolini, M.; Speroni, G. P. *J. Am. Chem. Soc.* **1965**, *87*, 3102.